

ORIGINAL ARTICLE

Assessment of metabolic fluxes in the mouse brain *in vivo* using ^1H - ^{13}C NMR spectroscopy at 14.1 Tesla

Lijing Xin^{1,2}, Bernard Lanz¹, Hongxia Lei^{3,4} and Rolf Gruetter^{1,3,5}

^{13}C magnetic resonance spectroscopy (MRS) combined with the administration of ^{13}C labeled substrates uniquely allows to measure metabolic fluxes *in vivo* in the brain of humans and rats. The extension to mouse models may provide exclusive prospect for the investigation of models of human diseases. In the present study, the short-echo-time (TE) full-sensitivity ^1H - ^{13}C MRS sequence combined with high magnetic field (14.1 T) and infusion of $[\text{U-}^{13}\text{C}_6]$ glucose was used to enhance the experimental sensitivity *in vivo* in the mouse brain and the ^{13}C turnover curves of glutamate C4, glutamine C4, glutamate+glutamine C3, aspartate C2, lactate C3, alanine C3, γ -aminobutyric acid C2, C3 and C4 were obtained. A one-compartment model was used to fit ^{13}C turnover curves and resulted in values of metabolic fluxes including the tricarboxylic acid (TCA) cycle flux V_{TCA} ($1.05 \pm 0.04 \mu\text{mol/g}$ per minute), the exchange flux between 2-oxoglutarate and glutamate V_x ($0.48 \pm 0.02 \mu\text{mol/g}$ per minute), the glutamate-glutamine exchange rate V_{gln} ($0.20 \pm 0.02 \mu\text{mol/g}$ per minute), the pyruvate dilution factor K_{dil} (0.82 ± 0.01), and the ratio for the lactate conversion rate and the alanine conversion rate $V_{\text{Lac}}/V_{\text{Ala}}$ (10 ± 2). This study opens the prospect of studying transgenic mouse models of brain pathologies.

Journal of Cerebral Blood Flow & Metabolism (2015) **35**, 759–765; doi:10.1038/jcbfm.2014.251; published online 21 January 2015

Keywords: energy metabolism; glucose; glutamate; lactate; MR spectroscopy

INTRODUCTION

In vivo ^{13}C magnetic resonance spectroscopy (MRS) in conjunction with the administration of ^{13}C labeled glucose provides a unique tool to assess cerebral metabolism noninvasively. For instance, following the infusion of $[\text{1-}^{13}\text{C}]$ or $[\text{1,6-}^{13}\text{C}_2]$ glucose, ^{13}C MRS can dynamically monitor the ^{13}C label incorporation into desired carbon positions of MR detectable metabolites, e.g., glutamate (Glu) and glutamine (Gln). Then, cerebral metabolic fluxes can be quantitatively derived from experimentally measured ^{13}C -label time courses using a mathematical model.^{1–3}

Mice have been widely used for genetic modification to investigate the pathology of respective human diseases. The use of ^{13}C MRS studies on transgenic mouse models may provide unique insights into the pathologies of various brain diseases. For instance, the pathogenesis of Huntington's disease may involve the impairment of glutamate-glutamine cycling⁴ assessed uniquely by ^{13}C MRS. *In vivo* ^{13}C MRS is commonly conducted in the human⁵ and rat brain.⁶ However, for the mouse brain, the intrinsically low sensitivity of ^{13}C MRS and the small brain size render the measurement of ^{13}C labeling into metabolites *in vivo* challenging. Hence, most ^{13}C MRS studies in mouse brain were achieved by using brain extracts.^{7,8} One *in vivo* ^{13}C study in mouse brain, using direct ^{13}C MRS by image selected *in vivo* spectroscopy localization with distortionless enhancement by polarization

transfer, reported time courses of C4 and C3 of Glu and Gln.⁹ However, the cerebral metabolic fluxes remain to be determined.

In addition, a time-resolved isotopic enrichment of plasma glucose is typically required as an input function to derive metabolic fluxes from ^{13}C labeled time courses using a given metabolic model in a ^{13}C labeled glucose infusion study. However, frequent blood sampling in small animals such as mouse during ^{13}C NMR experiment is hardly feasible due to the small blood volume of the mouse and rather big dead volume in the catheter from the center of the magnet to the entrance of the magnet bore.

Relative to direct ^{13}C MRS techniques, indirect detection of ^{13}C through ^1H combined with $[\text{1,6-}^{13}\text{C}_2]$ or $[\text{U-}^{13}\text{C}_6]$ glucose administration can improve the sensitivity and allow the direct measurement of fractional enrichments (FEs). However, the distinct separation of ^{13}C labeling in Glu and Gln using indirect detection requires sufficiently high spectral resolution.¹⁰ Recently, a short-echo-time (TE) full-sensitivity ^1H - ^{13}C NMR sequence was proposed and validated at a high magnetic field strength of 14.1 T, which provides high spectral resolution and signal sensitivity.¹¹

Therefore, the aim of the present study was to use the short-TE full-sensitivity ^1H - ^{13}C MRS¹¹ combined with high magnetic field (i.e., 14.1 T) and infusion of $[\text{U-}^{13}\text{C}_6]$ glucose to measure the time-resolved ^{13}C labeling of individual metabolites with a focus on glutamate and glutamine, to assess metabolic fluxes *in vivo* in the mouse brain.

¹Laboratory of Functional and Metabolic Imaging (LIFMET), Ecole Polytechnique Fédérale de Lausanne, Lausanne, Switzerland; ²Unit for Research in Schizophrenia, Department of Psychiatry, Center for Psychiatric Neuroscience, Lausanne University Hospital (CHUV), Lausanne, Switzerland; ³Department of Radiology, University of Geneva, Geneva, Switzerland; ⁴Animal Imaging and Technology Core (AIT), Center for Biomedical Imaging (CIBM), Ecole Polytechnique Fédérale de Lausanne, Lausanne, Switzerland and ⁵Department of Radiology, University of Lausanne, Lausanne, Switzerland. Correspondence: Drs L Xin and H Lei, Ecole Polytechnique Fédérale de Lausanne (EPFL), SB—LIFMET, CH F0 632, Station 6, Lausanne 1015, Switzerland.

E-mail: lijing.xin@epfl.ch, hongxia.lei@epfl.ch

This work was supported by Centre d'Imagerie BioMédicale (CIBM) of the UNIL, UNIGE, HUG, CHUV, and EPFL, the Leenaards, Jeantet Foundations and Swiss National Science Foundation grant SNF 3100A0-149983.

Received 25 August 2014; revised 27 November 2014; accepted 15 December 2014; published online 21 January 2015

MATERIALS AND METHODS

Animal Preparation

Male ICR-CD mice (33.4 ± 3.7 g, $n = 5$, Charles River, L'Arbresle Cedex, France) were housed in standard cages, fasted over 7 hours with free access to water and anesthetized using isoflurane (1% to 2%) mixed with O₂. One femoral vein was cannulated for the infusion of [U-¹³C₆] glucose (Sigma-Aldrich, St. Louis, MO, USA). After giving a bolus of a 20% (w/v) 99%-enriched [U-¹³C₆] glucose solution at an exponentially decaying rate over 5 minutes, a 67%-enriched [U-¹³C₆] glucose solution was infused continuously for up to 3 hours.^{12,13} The respiration rate was continuously monitored (SA Instruments Inc., Stony Brook, NY, USA) and maintained in the range of 80 to 110 breath per minute by adjusting the amount of isoflurane in the O₂ to sustain mouse under physiological condition, i.e., pH=7.3 to 7.4, PaCO₂=30 to 42 mm Hg and PaO₂>100 mm Hg (data not shown), all of which allowed sustaining normal functional activity and normal cerebral blood flow.^{14,15} The mouse was placed in a holder (RAPID Biomedical GmbH, Rimpar, Germany) and the head was stereotaxically fixed. Body temperature was measured by a rectal thermosensor and maintained at $36.0 \pm 0.5^\circ\text{C}$ with the circulation of heated water. All animal preparation procedures were performed in accordance with local and federal guidelines (EXANIM, Expérience sur animaux-SCAV, Service de la consommation et des affaires vétérinaires, Switzerland) and were approved by the Veterinary Office of Canton de Vaud.

In Vivo NMR Spectroscopy

Magnetic resonance spectroscopy experiments were performed in a 14.1 T magnet with a 26 cm horizontal bore (Agilent Technologies, Palo Alto, CA, USA) using a homebuilt geometrically decoupled ¹H quadrature surface coil (13 mm diameter) and a linearly polarized ¹³C coil (10 mm diameter) as a transceiver. Images for voxel positioning were obtained using a multislice fast spin-echo sequence in sagittal and coronal planes (effective TE=54 ms, repetition time=4,000 ms, echo train length=8, average=4, slice thickness=0.6 mm, slices=25, field of view=20×20 mm², data matrix=256×256). ¹³C decoupled ¹H MR spectra were acquired using a previously proposed full signal intensity ¹H-[¹³C] NMR sequence 'SPECIAL-BISEP' (Supplementary Figure S1),¹¹ which was a hybrid sequence composed of SPECIAL (SPin Echo, full Intensity Acquired Localized spectroscopy) localization part¹⁶ and a preceding ¹³C editing block based on the inversion B₁-insensitive spectral editing pulse (BISEP), including a segmented 0° BIR-4 pulse with two pulse interval delays ($\tau = 1/2J$) in the ¹H channel and an adiabatic full passage (AFP) in the ¹³C channel centered at the central segment of the 0° BIR-4 pulse.¹⁷ ¹³C editing was achieved by turning on and off the AFP pulse in the ¹³C channel on alternate scans, and then the edited spectrum (i.e., ¹³C AFP off-¹³C AFP on) contained ¹³C coupled ¹H resonances. Outer volume suppression and water suppression with VAPOR (VARIABLE Pulse power and Optimized Relaxation delays)¹⁸ were applied before SPECIAL-BISEP. B₀

inhomogeneity was optimized using first- and second-order shimming with FAST(EST)MAP,^{19,20} resulting in water linewidth of 24 to 28 Hz for a volume of 60 μL ($5 \times 4 \times 3$ mm³) containing primarily cerebral cortex and striatum (Figure 2). Adiabatic ¹³C decoupling¹⁰ was applied during 145 ms acquisition time. Spectra with ¹³C AFP off and on were acquired with 8-scan blocks in an interleaved mode (TE=2.8 ms, repetition time=4 seconds) during the whole infusion experiment.

Data Analysis

After Fourier transformation and frequency correction, every four blocks (64 averages) of spectra were summed and quantified with LCMoDel (Stephen Provencher Inc., Oakville, ON, Canada).²¹ Nonedited ¹H spectra acquired with ¹³C AFP off, which contain ¹H resonances coupled to both ¹³C and ¹²C nuclei, were quantified with a standard ¹H MRS basis set containing a measured macromolecular baseline²² and simulated metabolite spectra.²³ Another basis set including simulated metabolite spectra of ¹H resonances coupled to *N*-acetyl aspartate (NAA) C6, Glu (C2, C3, and C4), Gln (C2, C3, and C4), γ -aminobutyric acid (GABA) (C2, C3, and C4), aspartate (Asp) (C2 and C3), glucose (C2-C6), total creatine (C2 and C3), lactate (Lac) C3, and alanine (Ala) C3 was used to quantify ¹³C edited MR spectra. All metabolites concentrations were calculated using total creatine as an internal reference by assuming its concentration of 8 μmol/g.²⁴

Metabolic Modeling

In the metabolic reaction chain of glucose utilization in brain tissue, pyruvate (Pyr) is the last intermediate of the glycolysis and is not only a precursor for oxidative metabolism in the tricarboxylic acid (TCA) cycle, but also of lactate and alanine. Given the strong activity of lactate dehydrogenase allowing fast exchange between pyruvate and lactate as compared with the TCA cycle rate,^{25,26} the ¹³C turnover of LacC3 closely follows that of PyrC3 in terms of ¹³C FE. On the time scale of the ¹³C turnover of the amino acids labeled through the TCA cycle, the FE of LacC3 can therefore be used as an input function of the metabolic system, as a substitute to the nonmeasurable pool of pyruvate. The LacC3 turnover curve was thus smoothed by being fitted with an exponential function $FE(t) = (a \cdot t + b)(1 - e^{-c \cdot t})$ and used as the input function for the metabolic model. Cerebral metabolic fluxes were explored by fitting a one-compartment metabolic model of mitochondrial metabolism (Figure 1A)^{2,27} to the measured ¹³C labeling time courses of metabolites (i.e., GluC4, GlnC4, GluC3+GlnC3 (GlxC3) and AspC2). The curve fitting process was undertaken in MATLAB (Version 7.11, The MathWorks, Inc., Natick, MA, USA) using a standard built-in ordinary differential equation solver and a modified Levenberg-Marquardt nonlinear regression method. The fitting procedure was weighted with the square root of the inverse of the variance of the experimental noise, to compensate for the different precisions in the measurement of the turnover curves.

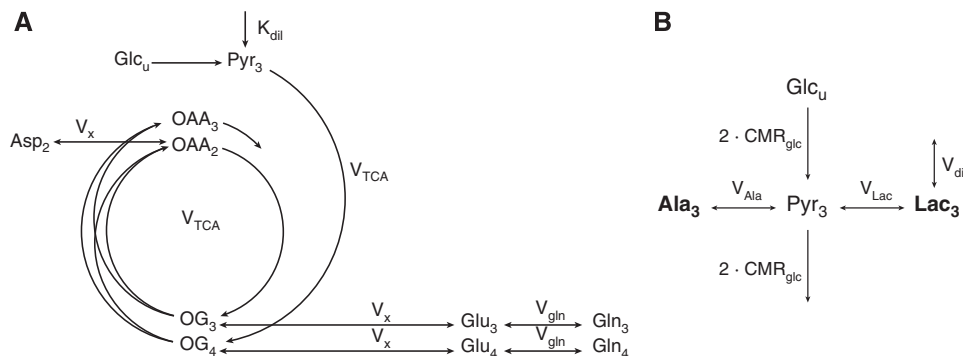


Figure 1. (A) Scheme of the mathematical model used to describe ¹³C label incorporation into cerebral metabolites during ¹³C labeled glucose infusion. ¹³C label derived from ¹³C labeled glucose is incorporated into C3 of pyruvate. Through pyruvate dehydrogenase ¹³C label enters the tricarboxylic acid (TCA) cycle and labels C4 position of 2-oxoglutarate (OG) in the first TCA cycle turn. Via trans-mitochondrial transport OG exchanges with cytosolic glutamate (Glu) which gets labeled at position C4. In the second turn of TCA cycle, OG C3 receives the label from OG C4 and Glu C3 gets further labeled. Aspartate (Asp) gets labeled via the trans-mitochondrial exchange with TCA cycle intermediate oxaloacetate (OAA). C4 and C3 positions of glutamine (Gln) accumulate labels from Glu C4 and C3 through Glu-Gln cycle. V_{TCA} , the TCA cycle rate; V_x , exchange flux between mitochondrial TCA cycle intermediates and cytosolic glutamate; V_{gln} , glutamate-glutamine exchange rate; K_{dil} , the dilution factor of the lactate (Lac)/pyruvate pool induced by uptake of unlabeled plasma lactate. (B) Scheme of the metabolic model for the ¹³C labeling of AlaC3 and LacC3 from ¹³C labeled glucose. V_{Lac} , lactate conversion rate; V_{Ala} , alanine conversion rate; CMR_{glc} , cerebral metabolic rate of glucose consumption; V_{dil} , dilution flux in the lactate pool induced by uptake of unlabeled plasma lactate. All subscript numbers represent ¹³C labeled carbon position.

In a second step, the ratio of lactate conversion rate V_{Lac} and alanine conversion rate V_{Ala} was obtained by fitting time courses of AlaC3 and LacC3 to a compartmental model (Figure 1B) of the chemical reactions involving pyruvate in brain glucose metabolism. In this model, the FE of glucose is assumed to follow a step function at a level of 67% after the start of tracer infusion, as previously shown using this type of infusion protocol.^{12,13} The cerebral metabolic rate of glucose consumption (CMR_{glc}) was fixed to $0.5 \mu\text{mol/g}$ per minute, which is a representative value for brain glucose metabolism in anesthetized mice, as found in this study and in the literature.⁷ In the case of the considered model, with a bidirectional flux with the same pyruvate pool, the FE of Lac is expected to be very close to the FE of Ala, since the dilution flux in lactate also dilutes the labeling in Ala through the exchange with Pyr. Note that the calculated FE of AlaC3 was slightly higher than that of LacC3, which may be ascribed to a potential underestimation of the small Ala concentration given its overlap with macromolecule resonances at 1.4 ppm. Therefore, the FE turnover curve of AlaC3 at steady state was scaled with the FE of LacC3, based on the ratio between FELacC3/FEAlaC3 at steady state found in brain extracts in Duarte *et al*.¹³ The errors of all adjusted metabolic fluxes were evaluated by Monte-Carlo simulation.

The equations describing the mathematical modeling approaches used in this study are reported in appendix, as Supplementary information.

RESULTS

Nonedited (Figure 2A) and edited ¹H MR spectra (Figure 2B) acquired from the volume of interest of $60 \mu\text{L}$ in the mouse brain using SPECIAL-BISEP show good spectral quality at 14.1 T in this study, such as high spectral resolution, e.g., the separation of GluC4 and GlnC4, and the absence of contamination signal from extraneous lipids, which allows the measurement of lactate and alanine. In the ¹³C edited spectra, ¹³C labeled ¹H resonances in the mouse brain can be observed in LacC3, AlaC3, GluC4, GlnC4, GlxC3, GlxC2(GluC2+GlnC2), AspC3, AspC2, GABAC3, GABAC2, and Glc(C2-C6) (Figure 2B).

To show the dynamic incorporation of ¹³C label into individual carbon positions of metabolites, edited spectra containing ¹³C-coupled ¹H resonances were summed over 5 minutes for 90 minutes after the start of [¹³C₆] glucose infusion (Figure 3). Note that ¹³C labeling into Glc and Lac can already be observed during

the second 5-minute acquisition after the start of infusion. Subsequently, carbon positions of Ala, Glu, Gln and GABA were labeled, respectively (Figure 3).

To determine the total concentration of metabolites (¹³C+¹²C) and the concentrations of ¹³C labeled metabolites, nonedited and edited ¹H spectra were analyzed using LCModel. The pool sizes of glutamate ($9.1 \pm 0.5 \mu\text{mol/g}$, mean \pm s.e.m.), glutamine ($3.4 \pm 0.1 \mu\text{mol/g}$), and aspartate ($2.1 \pm 0.2 \mu\text{mol/g}$) were measured simultaneously from the nonedited ¹H spectra. The average time courses of ¹³C labeled GluC4, GlnC4, GlxC3, AspC2 and GABA(C2, C3, and C4) concentration were obtained from the edited spectra with a temporal resolution of 4.3 minutes during 180-minute infusion of [¹³C₆] glucose (Figure 4).

To determine the TCA cycle flux ($V_{TCA} = 1.05 \pm 0.04 \mu\text{mol/g}$ per minute, mean \pm s.d.), the exchange flux between 2-oxoglutarate (mitochondrial TCA cycle intermediate) and glutamate (cytosolic amino acid) ($V_x = 0.48 \pm 0.02 \mu\text{mol/g}$ per minute), the Glu-Gln exchange rate ($V_{gln} = 0.20 \pm 0.02 \mu\text{mol/g}$ per minute) and the dilution factor ($K_{dil} = 0.82 \pm 0.01$), the average time courses of GluC4, GlnC4, GlxC3, and AspC2 were fitted by a one-compartment model of mitochondrial metabolism using fitted LacC3 time course as the input function (Figures 4A–4C). The comparison of metabolic fluxes obtained in mouse (*ex vivo*), rat, and human (*in vivo*) brains is summarized in Table 1.

To determine the ratio of V_{Lac}/V_{Ala} (10 ± 2), the turnover curves of LacC3 and AlaC3 (Figure 5A) were fitted, assuming a glucose utilization CMR_{glc} of $0.5 \mu\text{mol/g}$ per minute.⁷ To investigate the effect of the assumed CMR_{glc} value on the assessment of V_{Lac}/V_{Ala} ratio, V_{Lac}/V_{Ala} ratios were calculated by varying CMR_{glc} values (Figure 5B). For CMR_{glc} values lower than $0.45 \mu\text{mol/g}$ per minute, the simulated curves failed to describe the initial rising portion of the measured LacC3 enrichment curve. This value was therefore used as a minimum in the analysis. Error bars represents the standard deviation determined by Monte-Carlo simulations. The V_{Lac}/V_{Ala} ratio was found to be between 6.6 and 11.6 for the considered CMR_{glc} range. For an assumed value of CMR_{glc} of $0.5 \mu\text{mol/g}$ per minute,⁷ the ratio was 10 ± 2 . The pool size of Ala and Lac may vary due to physiological conditions, such as the

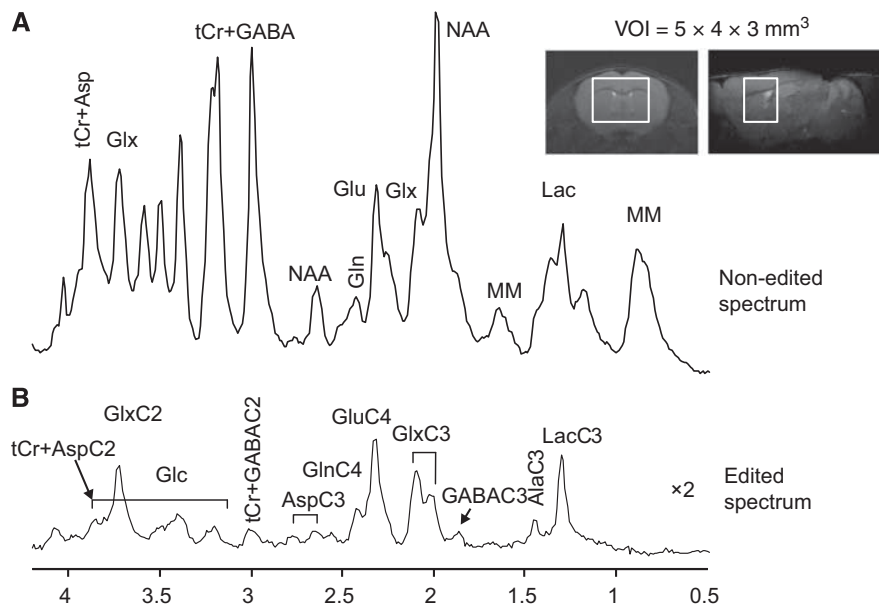


Figure 2. Representative coronal and sagittal fast spin-echo images of the mouse brain with the volume of interest (VOI) for magnetic resonance spectroscopy (MRS) measurement. Averaged nonedited (A) and edited (B) ¹H magnetic resonance (MR) spectra acquired in the mouse brain during first hour of [¹³C₆] glucose infusion (VOI = $60 \mu\text{L}$, nt = 960, no apodization was applied). Ala, alanine; Asp, aspartate; GABA, γ -aminobutyric acid; Glc, glucose; Gln, glutamine; Glu, glutamate; Glx, Glu+Gln; Lac, lactate; MM, macromolecules; NAA, N-acetyl aspartate; tCr, total creatine.

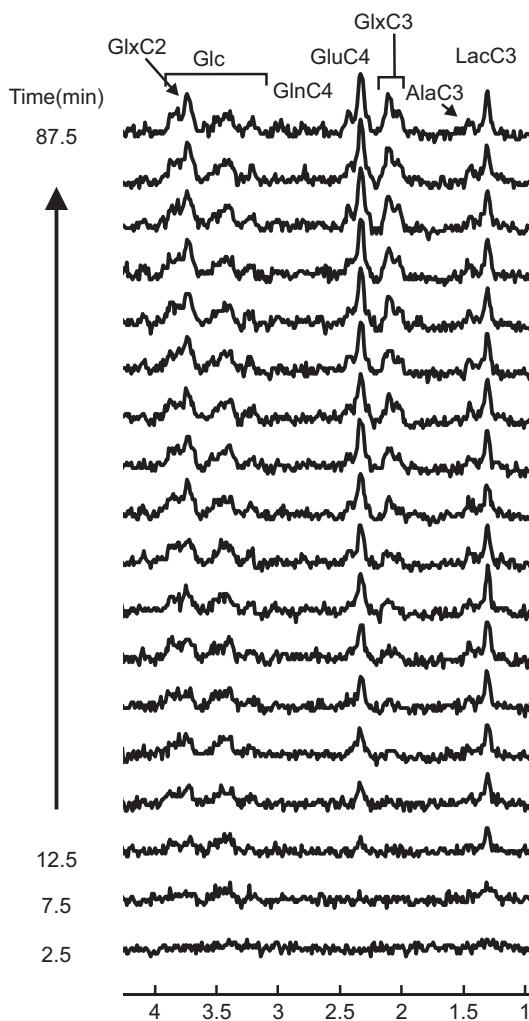


Figure 3. Stack plot of ^{13}C labeling incorporation into cerebral metabolites during the first 90 minutes of $[\text{U-}^{13}\text{C}_6]$ glucose infusion with time resolution of 5 minutes. No baseline correction and water signal removal were applied.

higher plasma glucose level during $[\text{U-}^{13}\text{C}_6]$ glucose infusion. From the ^1H MRS data, we observed a net production of lactate ($0.01 \mu\text{mol/g}$ per minute) and in a smaller extent of alanine ($0.002 \mu\text{mol/g}$ per minute). When this metabolic nonsteady-state condition was added to the metabolic model, i.e., considering linearly increasing pool sizes, no statistically significant difference was found for the $V_{\text{Lac}}/V_{\text{Ala}}$ ratio (data not shown).

DISCUSSION

The present study measures for the first time *in vivo* in the mouse brain the ^{13}C label incorporation into brain metabolites using $^1\text{H-}^{13}\text{C}$ MRS with the concomitant determination of the TCA cycle flux V_{TCA} , the exchange flux between 2-oxoglutarate and glutamate V_{Gln} , the Glu-Gln exchange rate V_{Gln} , the pyruvate dilution factor K_{dil} and the ratio $V_{\text{Lac}}/V_{\text{Ala}}$.

$^1\text{H-}^{13}\text{C}$ Magnetic Resonance Spectroscopy in the Mouse Brain

Due to the small size of the mouse brain and the intrinsic low sensitivity of ^{13}C MRS, several strategies were used in this study to enhance sensitivity of the measurement. The use of $[\text{U-}^{13}\text{C}_6]$ glucose infusion increased the sensitivity of the measurement by two-fold relative to $[\text{1-}^{13}\text{C}]$ glucose by labeling both molecules of

$[\text{3-}^{13}\text{C}]$ pyruvate from $[\text{U-}^{13}\text{C}_6]$ glucose through glycolysis. In addition, as an alternative to direct-detected ^{13}C MRS,⁹ detection of ^{13}C labeling through coupled ^1H nuclei intrinsically increased the experimental sensitivity. The application of SPECIAL-BISEP¹¹ at ultra-high magnetic field of 14.1 T further increased the quality of *in vivo* spectra from the mouse brain in terms of signal-to-noise ratio, spectral resolution, and localization performance. Moreover, the nonedited ^1H spectra allow the straightforward measurement of metabolites pool size *in vivo*, which is especially practical for recording the pool size of those metabolites that may vary during the infusion experiment.^{13,28} Although the application of $^1\text{H-}^{13}\text{C}$ MRS at 14.1 T improved the spectral dispersion of GluC4 and GlnC4 (Figure 2B), the separation of labeling in C2 and C3 of Glu and Gln was not complete.

Input Function for Metabolic Modeling

As a major energy source of the brain, glucose is first transported into brain across the blood-brain barrier and then degraded into pyruvate by the glycolytic pathway. Pyruvate can then be transported into mitochondria and oxidized in the TCA cycle. It can also be converted to lactate through lactate dehydrogenase, which has a higher activity than that of the pyruvate dehydrogenase.²⁵

Therefore, following the glucose metabolic pathway, several candidates, e.g., plasma glucose, brain glucose, lactate, and pyruvate could serve as an input function in the mathematic modeling to derive metabolic fluxes. However, due to small pool size of pyruvate, it can only be detected with sensitivity enhancement using dynamic nuclear polarization.²⁹

To date, when using direct ^{13}C MRS, it has been hardly feasible to measure the time-resolved FE of metabolic pools such as glucose or lactate *in vivo*. Therefore, a time-resolved FE of plasma glucose was commonly obtained from blood sampling during the MRS experiment and then used as an input function to derive metabolic fluxes using a given metabolic model in a ^{13}C labeled glucose infusion study.^{13,30} However, frequent blood sampling during ^{13}C NMR experiments remains challenging in the mouse due to its small blood volume. Recently, one study showed the blood sampling during ^{13}C MR experiments in young rat (~100 g) by using a specifically designed animal holder.³¹

Alternatively, the measure of FE of brain glucose using $^1\text{H-}^{13}\text{C}$ MRS has been reported in the rat brain;¹⁰ however, this remains challenging as it heavily relies on excellent water suppression and shimming performance. The optimization of field inhomogeneity in mouse brain is highly demanding on shimming capacity because of an increased susceptibility gradient comparing with rat brain²⁴ and becomes even more challenging at 14.1 T compared with 9.4 T.³² Therefore, in the current study, the reliable measurement of C1 glucose at 5.2 ppm was not applicable in mouse brain. Other ^1H resonances coupled to C2-C6 of glucose present a number of peaks (3.3 to 3.8 ppm) overlapping with macromolecule baseline and many metabolites. This results in the underestimation of total glucose concentration in the nonedited spectra and overestimation of FE of brain glucose. Therefore, brain glucose might not be best candidate as the input function in this study.

However, the mouse brain contains higher level of lactate (3 to 5 mmol/L)^{24,33} across four brain regions relative to rats (1 to 2 mmol/L)³⁴ and human (~1 mmol/L),³⁵ leading to direct time course measurements of lactate FE using $^1\text{H-}^{13}\text{C}$ MRS (Figure 4C). Compared with plasma or brain glucose, which is several biochemical steps further from the TCA cycle, the lactate pool is likely to represent closely the FE of pyruvate. In addition, lactate can also be transported into the brain via monocarboxylate transporters and utilized as brain fuel.³⁶ The use of lactate as an input function could take into account the potential ^{13}C labeling from the blood. Therefore, the brain lactate signal is the most favourable and straightforward candidate for input function in the mouse brain.

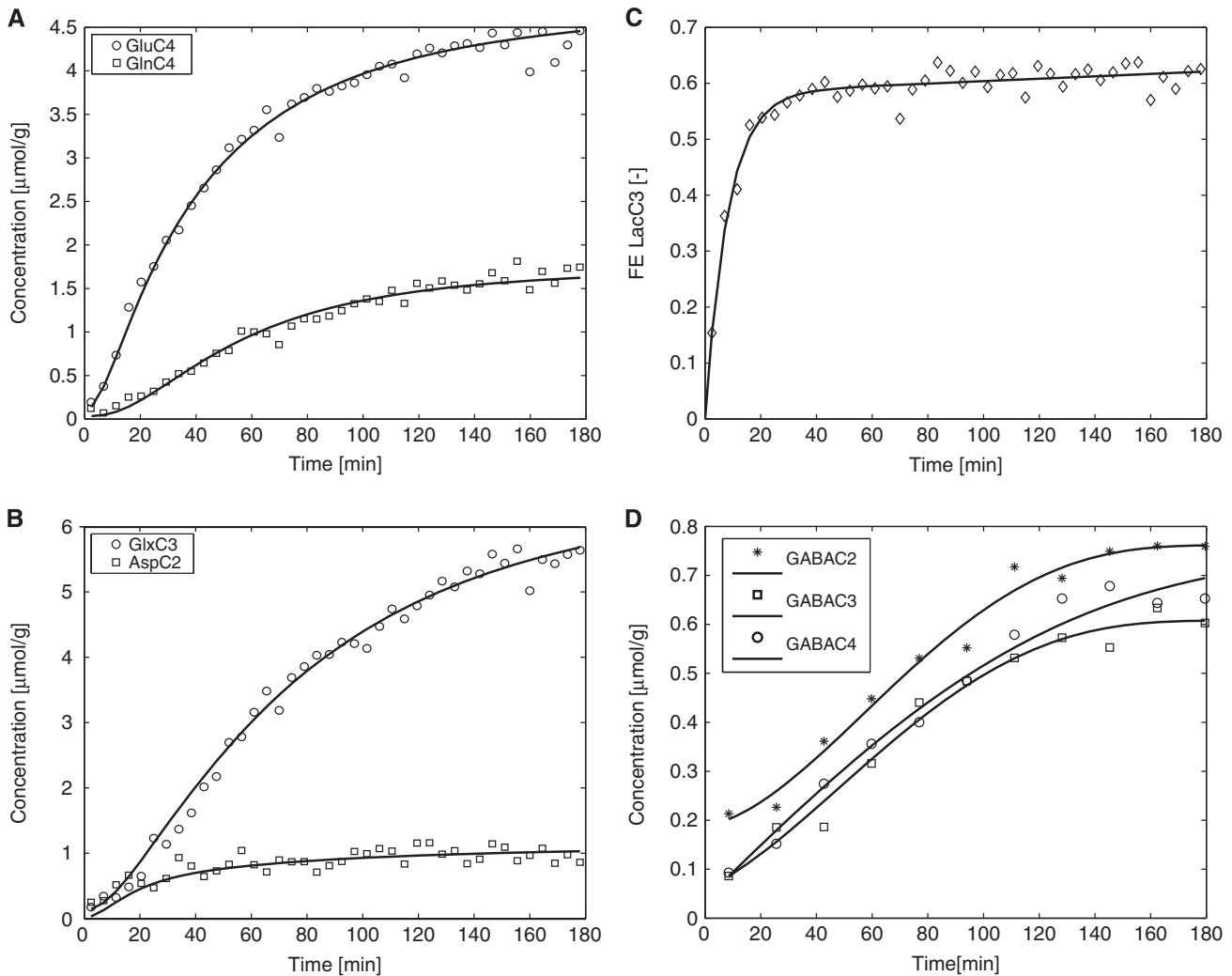


Figure 4. Average time courses of (A) GlnC4 (□) and GluC4 (○), (B) GlxC3 (○) and AspC2 (□), (C) LacC3, and (D) GABA C2(*), C3(□), and C4(○) during 180-minute [U-¹³C₆] glucose infusion (*n* = 5). LacC3 time course was fitted with an exponential function. The fitting curves of GluC4, GlnC4, GlxC3, and AspC2 were the best fit obtained from one-compartment metabolic modeling. Spectra were average over 17 minutes for time courses of GABA C2, C3, and C4. Polynomial function was used to fit GABA C2, C3, and C4 for visualization purpose. Asp, aspartate; Gln, glutamine; Glu, glutamate; Lac, lactate.

Table 1. Metabolic fluxes (μmol/g per minute, mean ± s.d.) obtained in rat, human, and mouse brain using ¹³C MRS

	V_{TCA}^n	V_{TCA}	V_x	V_{NT}	V_g	V_{PC}	Anesthetic	VOI location	Reference
Rat ^a	0.44 ± 0.01	0.74 ± 0.02	0.76 ± 0.07 ^b	0.12 ± 0.01	0.23 ± 0.02	0.07 ± 0.01	α-Chloralose	Whole brain	Duarte <i>et al</i> ¹³
Rat ^c	0.37 ± 0.06	0.73 ± 0.06	0.46 ± 0.05 ^b	0.15 ± 0.01	0.27 ± 0.02	0.09 ± 0.01	α-Chloralose	Cortex	Lanz <i>et al</i> ³⁷
Rat ^d	–	0.71 ± 0.02	0.88 ± 0.08	–	–	–	α-Chloralose	Whole brain	Henry <i>et al</i> ¹²
Rat ^a	0.79 ± 0.15	0.93 ± 0.15	9.6 ± 6.9	0.31 ± 0.07	0.04 ^e	0.096 ^e	Halothane	Gray matter	de Graaf <i>et al</i> ⁶
Rat ^a	0.20 ± 0.11	0.31 ± 0.11	6.4 ± 3.8	0.02 ± 0.04	0.01 ^e	0.096 ^e	Halothane	White matter	de Graaf <i>et al</i> ⁶
Rat ^a	0.42 ± 0.09	0.54 ± 0.09	6.7 ± 4.1	0.18 ± 0.12	0.02 ^e	0.096 ^e	Halothane	Subcortex	de Graaf <i>et al</i> ⁶
Human ^d	–	0.80 ± 0.10	–	–	–	–	–	Gray matter	Mason <i>et al</i> ³⁹
Human ^d	–	0.17 ± 0.01	–	–	–	–	–	White matter	Mason <i>et al</i> ³⁹
Human ^d	–	0.73 ± 0.19	57 ± 26	0.47 ± 0.70	–	–	–	Occipital-parietal	Mason <i>et al</i> ⁴⁰
Human ^d	0.57 ± 0.06	0.72 ± 0.07	0.57 ± 0.19	0.17 ± 0.05	0.06 ± 0.04	0.09 ± 0.02	–	Visual cortex	Gruetter <i>et al</i> ³⁸
Mouse ^f	0.91 ± 0.05	1.06 ± 0.07	99.96	0.36 ± 0.02	0.13 ± 0.04	0.02 ± 0.03	Halothane	Cortex extract	Tiwari <i>et al</i> ⁷
Mouse ^f	0.75 ± 0.05	0.83 ± 0.07	99.96	0.18 ± 0.01	0.02 ± 0.04	0.06 ± 0.03	Halothane	Striatum extract	Tiwari <i>et al</i> ⁷
Mouse ^g	–	1.05 ± 0.04	0.48 ± 0.02	0.20 ± 0.02 ^h	–	–	Isoflurane	Cortex and striatum	Current study

Abbreviations: MRS, magnetic resonance spectroscopy; TCA, tricarboxylic acid; V_{TCA}^n , rate of neuronal TCA cycle; TCA cycle flux $V_{TCA} = V_{TCA}^n + V_g + V_{PC}$; V_g , rate of glial TCA cycle; V_{PC} , rate of pyruvate carboxylase; V_{NT} , apparent rate of glutamate neurotransmission; VOI, volume of interest. ^a[1,6-¹³C₂] glucose infusion. ^bExchange rate between 2-oxoglutarate and glutamate in neurons. ^c[2-¹³C] acetate infusion. ^d[1-¹³C] glucose infusion. ^eAssumed values. ^f*Ex vivo*, [1,6-¹³C₂] glucose and [2-¹³C] acetate infusion. ^g[U-¹³C₆] glucose infusion. ^h V_{NT} was set to V_{gln} in the one-compartment model.

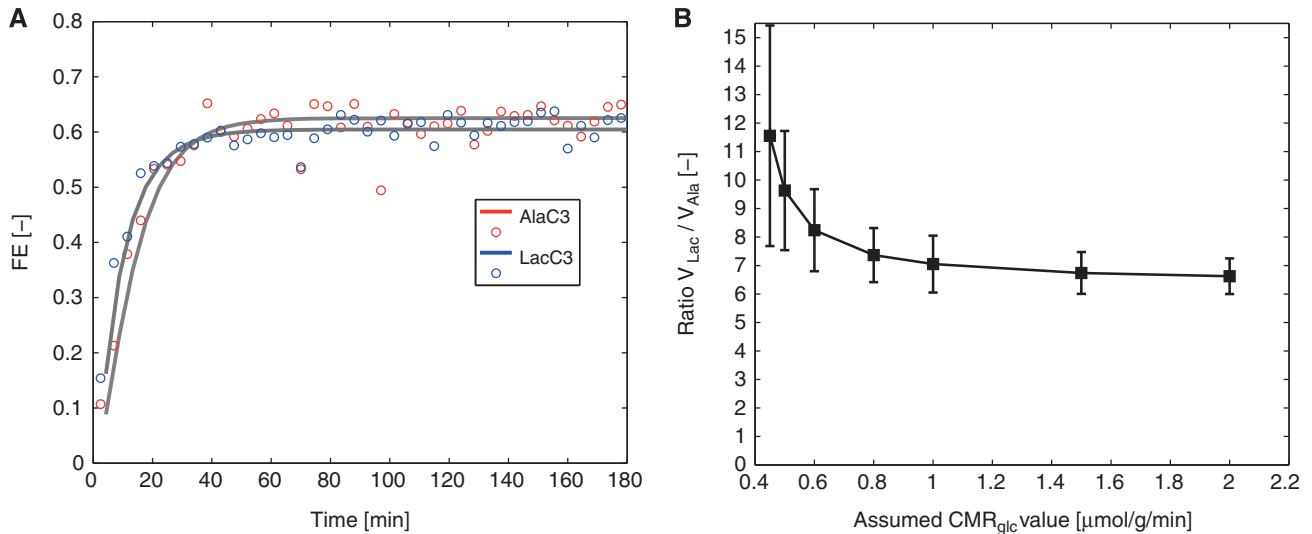


Figure 5. (A) Average time courses of AlaC3 and LacC3 ($n = 5$) were shown and fitted with a mathematical model to calculate $V_{\text{Lac}}/V_{\text{Ala}}$. (B) The effect of the assumed cerebral metabolic rate of glucose consumption (CMR_{glc}) value on the ratio of $V_{\text{Lac}}/V_{\text{Ala}}$. Ala, alanine; FE, fractional enrichment; Lac, lactate.

Metabolic Fluxes

The value of TCA cycle flux ($V_{\text{TCA}} = 1.05 \pm 0.04 \mu\text{mol/g}$ per minute) representing essentially glutamatergic neuron activity is in agreement with the results obtained from mouse brain extracts (Table 1).⁷ As shown in Table 1, mouse brains showed a higher TCA cycle flux compared with human and rat brain, suggesting distinct kinetics for the mouse. The Glu-Gln exchange rate of $0.20 \pm 0.02 \mu\text{mol/g}$ per minute for cerebral cortex and striatum falls in the range of reported *ex vivo* values of 0.18 ± 0.01 and $0.36 \pm 0.02 \mu\text{mol/g}$ per minute in striatum and cortex.⁷ The trans-mitochondrial flux V_x ($0.48 \pm 0.02 \mu\text{mol/g}$ per minute) summarizing the exchange between 2-oxoglutarate and cytosolic glutamate was measured for the first time in the *in vivo* mouse brain and was found on the same order of magnitude as the TCA cycle rate, similarly to previous studies in rats^{13,37} and humans.³⁸

In this study, we applied a one-compartment model analysis of brain energy metabolism based on the turnover curves GluC4, GlnC4, GlxC3, and AspC2. Since brain tissue is composed of many different cell types with distinct roles in energy metabolism, it would be desirable to develop the model into a more complex scheme closer to the tissue biochemical complexity. A next step would be to consider a two-compartment approach^{1,13,37} to distinguish between neuronal and astrocytic metabolism in the ¹³C labeling of glutamate, glutamine and aspartate. However, to characterize properly the activity of astrocytic and neuronal TCA cycles separately, the separate acquisition of the positions C4 and C3 of glutamate and glutamine is at least necessary,¹ when infusing [1,6-¹³C]glucose. The main reason is the different labeling pattern of the position C3 induced in the astrocytic compartment by the astrocytic-specific pyruvate carboxylase. This cell-specific labeling pattern enables to decouple the effects of neuronal and astrocytic TCA activity on the observed turnover curves by a gliat-specific dilution of glutamine C3. In the present study using [U-¹³C]glucose and limited to the measurement of GlxC3 due to spectral overlap, this cell-specific labeling pattern was not observed and the use of two-compartment modeling approach leads to strong correlations between the determined metabolic rates in the neuronal and astrocytic compartments (data not shown). This underdetermination can either be solved by fixing some metabolic rates using *a priori* knowledge or decreasing the level of complexity of the model, i.e., reducing it to a one-compartment approach. Future studies enabling the separate

measurement of the C3 and C2 positions of glutamate and glutamine are expected to give a cell-specific insight in cerebral oxidative metabolism in the mouse.

Metabolic concentrations, required for the determination of the metabolic fluxes, are commonly varying strongly with cerebral regions as shown in the human³⁵, rat,³⁴ and mouse²⁴ brains. Therefore, it is crucial to determine the metabolic pool size in the studied volume of interest (VOI). One of the advantages of ¹H-[¹³C] MRS is the simultaneous measurement of metabolic pool sizes from nonedited spectra. The metabolite values measured in the VOI containing mainly cerebral cortex and striatum in this study are in the range of those reported *in vivo* in the mouse striatum and cortex.²⁴

Metabolic Flux Ratio of $V_{\text{Lac}}/V_{\text{Ala}}$

In the present study, we report for the first time the *in vivo* measurement of ¹³C label incorporation into Lac and Ala in the mouse brain. A separate metabolic model of the biochemical reactions involving the production of alanine and lactate from pyruvate was therefore developed to enable the characterization of the dynamics of the labeling of alanine and lactate (Figure 1B). The conversion rate between pyruvate and alanine through alanine aminotransferase was expected to be on the same order of magnitude as the conversion between pyruvate and lactate. Therefore, the strategy of substituting the unknown FE time course of PyrC3 by the measured FE turnover curve of LacC3 as used for the modeling of the TCA cycle activity was not applicable. An alternative approach would be to work with another upstream substrate, such as the plasma glucose FE as an input function.

With the applied glucose infusion protocol, the FE of glucose in blood has been shown to reach steady state within 5 minutes.¹³ Blood glucose FE was therefore modeled as a step function. However, the biochemical pathways and intermediates from plasma glucose to cerebral pyruvate are numerous (i.e., glucose transport, phosphorylation, and glycolysis). All these intermediate labeling pools potentially delay the turnover of pyruvate as compared with blood glucose and therefore may affect the kinetics of ¹³C uptake in alanine and lactate. Since the glycolytic process is expected to be relatively slow compared with the conversion between pyruvate and lactate or alanine, this effect may not be negligible. Therefore, the separate evaluation of CMR_{glc} and the labeling fluxes V_{Ala} and V_{Lac} is not possible without

measuring the FE of PyrC3. However, since this labeling delay due to glycolysis affects pyruvate labeling, which is the last precursor for lactate and alanine, the dynamics of AlaC3 and PyrC3 turnover curves carries information on the relative conversion rates V_{Ala} and V_{Lac} , which could be determined in this study, as confirmed by Monte-Carlo simulation ($V_{Lac}/V_{Ala} = 10 \pm 2$).

In this study, a representative CMR_{glc} of $0.5 \mu\text{mol/g per minute}^7$ was assumed to avoid potential mathematical underdetermination of the metabolic model. Further analysis (Figure 5B) showed that assumed CMR_{glc} in a range of 0.45 to $2 \mu\text{mol/g per minute}$ resulted in a ratio V_{Lac}/V_{Ala} from 6.6 to 11.6. Note that the gradual increase in lactate and alanine concentrations measured by ^1H MRS did not affect the determination of the ratio V_{Lac}/V_{Ala} .

We conclude that high quality ^1H - ^{13}C NMR spectra can be acquired from a volume as small as $60 \mu\text{L}$ in mouse brain *in vivo* at 14.1 T. This allows to obtain ^{13}C labeling turnover curves of GluC4, GlnC4, GlxC3, and for the first time, AspC2, AlaC3, GABA (C2, C3, and C4) as well as LacC3 that offers precursor information to determine a number of metabolic fluxes without additional blood sampling. This study opens the prospect of studying transgenic mouse models of brain pathologies.

DISCLOSURE/CONFLICT OF INTEREST

The authors declare no conflict of interest.

REFERENCES

- Lanz B, Gruetter R, Duarte JM. Metabolic flux and compartmentation analysis in the brain. *Front Endocrinol* 2013; **4**: 156.
- Henry PG, Adriany G, Deelchand D, Gruetter R, Marjanska M, Oz G *et al*. In vivo ^{13}C NMR spectroscopy and metabolic modeling in the brain: a practical perspective. *Magn Reson Imaging* 2006; **24**: 527–539.
- Gruetter R, Adriany G, Choi IY, Henry PG, Lei H, Oz G. Localized in vivo ^{13}C NMR spectroscopy of the brain. *NMR Biomed* 2003; **16**: 313–338.
- Behrens PF, Franz P, Woodman B, Lindenberg KS, Landwehrmeyer GB. Impaired glutamate transport and glutamate-glutamine cycling: downstream effects of the Huntington mutation. *Brain* 2002; **125**: 1908–1922.
- Gruetter R, Novotny EJ, Boulware SD, Mason GF, Rothman DL, Shulman GI *et al*. Localized ^{13}C NMR spectroscopy in the human brain of amino acid labeling from D-[1- ^{13}C]glucose. *J Neurochem* 1994; **63**: 1377–1385.
- deGraaf RA, Mason GF, Patel AB, Rothman DL, Behar KL. Regional glucose metabolism and glutamatergic neurotransmission in rat brain in vivo. *Proc Natl Acad Sci USA* 2004; **101**: 12700–12705.
- Tiwari V, Ambadipudi S, Patel AB. Glutamatergic and GABAergic TCA cycle and neurotransmitter cycling fluxes in different regions of mouse brain. *J Cereb Blood Flow Metab* 2013; **33**: 1523–1531.
- Chowdhury GM, Gupta M, Gibson KM, Patel AB, Behar KL. Altered cerebral glucose and acetate metabolism in succinic semialdehyde dehydrogenase-deficient mice: evidence for glial dysfunction and reduced glutamate/glutamine cycling. *J Neurochem* 2007; **103**: 2077–2091.
- Nabuurs CI, Klomp DW, Veltien A, Kan HE, Heerschap A. Localized sensitivity enhanced in vivo ^{13}C MRS to detect glucose metabolism in the mouse brain. *Magn Reson Med* 2008; **59**: 626–630.
- Pfeuffer J, Tkac I, Choi IY, Merkle H, Ugurbil K, Garwood M *et al*. Localized in vivo ^1H NMR detection of neurotransmitter labeling in rat brain during infusion of [1- ^{13}C] D-glucose. *Magn Reson Med* 1999; **41**: 1077–1083.
- Xin L, Mlynarik V, Lanz B, Frenkel H, Gruetter R. ^1H -[^{13}C] NMR spectroscopy of the rat brain during infusion of [2- ^{13}C] acetate at 14.1 T. *Magn Reson Med* 2010; **64**: 334–340.
- Henry PG, Lebon V, Vaufrey F, Brouillet E, Hantraye P, Bloch G. Decreased TCA cycle rate in the rat brain after acute 3-NP treatment measured by in vivo ^1H -[^{13}C] NMR spectroscopy. *J Neurochem* 2002; **82**: 857–866.
- Duarte JM, Lanz B, Gruetter R. Compartmentalized cerebral metabolism of [1,6- ^{13}C]glucose determined by in vivo (^{13}C) NMR spectroscopy at 14.1 T. *Front Neuroenerg* 2011; **3**: 3.
- Takano T, Tian GF, Peng W, Lou N, Libionka W, Han X *et al*. Astrocyte-mediated control of cerebral blood flow. *Nat Neurosci* 2006; **9**: 260–267.
- Lei H, Pilloud Y, Magill AW, Gruetter R. Continuous arterial spin labeling of mouse cerebral blood flow using an actively-detuned two-coil system at 9.4T. *Conf Proc IEEE Eng Med Biol Soc* 2011; **2011**: 6993–6996.
- Mlynarik V, Gambarota G, Frenkel H, Gruetter R. Localized short-echo-time proton MR spectroscopy with full signal-intensity acquisition. *Magn Reson Med* 2006; **56**: 965–970.
- Garwood M, Merkle H. Heteronuclear spectral editing with adiabatic pulses. *J Magn Reson* 1991; **94**: 180–185.
- Tkac I, Starcuk Z, Choi IY, Gruetter R. In vivo ^1H NMR spectroscopy of rat brain at 1 ms echo time. *Magn Reson Med* 1999; **41**: 649–656.
- Gruetter R, Tkac I. Field mapping without reference scan using asymmetric echo-planar techniques. *Magn Reson Med* 2000; **43**: 319–323.
- Gruetter R. Automatic, localized in vivo adjustment of all first- and second-order shim coils. *Magn Reson Med* 1993; **29**: 804–811.
- Provencher SW. Estimation of metabolite concentrations from localized in vivo proton NMR spectra. *Magn Reson Med* 1993; **30**: 672–679.
- Kunz N, Cudalbu C, Mlynarik V, Huppi PS, Sizonenko SV, Gruetter R. Diffusion-weighted spectroscopy: a novel approach to determine macromolecule resonances in short-echo time ^1H -MRS. *Magn Reson Med* 2010; **64**: 939–946.
- Xin L, Gambarota G, Mlynarik V, Gruetter R. Proton T2 relaxation time of J-coupled cerebral metabolites in rat brain at 9.4 T. *NMR Biomed* 2008; **21**: 396–401.
- Tkac I, Henry PG, Andersen P, Keene CD, Low WC, Gruetter R. Highly resolved in vivo ^1H NMR spectroscopy of the mouse brain at 9.4 T. *Magn Reson Med* 2004; **52**: 478–484.
- Leong SF, Lai JC, Lim L, Clark JB. Energy-metabolizing enzymes in brain regions of adult and aging rats. *J Neurochem* 1981; **37**: 1548–1556.
- Xu S, Yang J, Shen J. In vivo ^{13}C saturation transfer effect of the lactate dehydrogenase reaction. *Magn Reson Med* 2007; **57**: 258–264.
- Uffmann K, Gruetter R. Mathematical modeling of (^{13}C) label incorporation of the TCA cycle: the concept of composite precursor function. *J Neurosci Res* 2007; **85**: 3304–3317.
- Deelchand DK, Shestov AA, Koski DM, Ugurbil K, Henry PG. Acetate transport and utilization in the rat brain. *J Neurochem* 2009; **109**: 46–54.
- Marjanska M, Iltis I, Shestov AA, Deelchand DK, Nelson C, Ugurbil K *et al*. In vivo ^{13}C spectroscopy in the rat brain using hyperpolarized [1-(^{13}C)]pyruvate and [2-(^{13}C)]pyruvate. *J Magn Reson* 2010; **206**: 210–218.
- de Graaf RA, Rothman DL, Behar KL. State of the art direct ^{13}C and indirect ^1H -[^{13}C] NMR spectroscopy in vivo. A practical guide. *NMR Biomed* 2011; **24**: 958–972.
- Ennis K, Deelchand DK, Tkac I, Henry PG, Rao R. Determination of oxidative glucose metabolism in vivo in the young rat brain using localized direct-detected (1) (^{13}C) NMR spectroscopy. *Neurochem Res* 2011; **36**: 1962–1968.
- Mlynarik V, Cudalbu C, Xin L, Gruetter R. ^1H NMR spectroscopy of rat brain in vivo at 14.1 Tesla: improvements in quantification of the neurochemical profile. *J Magn Reson* 2008; **194**: 163–168.
- Lei H, Berthet C, Hirt L, Gruetter R. Evolution of the neurochemical profile after transient focal cerebral ischemia in the mouse brain. *J Cereb Blood Flow Metab* 2009; **29**: 811–819.
- Tkac I, Rao R, Georgieff MK, Gruetter R. Developmental and regional changes in the neurochemical profile of the rat brain determined by in vivo ^1H - ^1H NMR spectroscopy. *Magn Reson Med* 2003; **50**: 24–32.
- Emir UE, Auerbach EJ, Moortele PF, Marjanska M, Ugurbil K, Terpstra M *et al*. Regional neurochemical profiles in the human brain measured by (1) H MRS at 7 T using local B(1) shimming. *NMR Biomed* 2011; **25**: 152–160.
- Boumezeur F, Petersen KF, Cline GW, Mason GF, Behar KL, Shulman GI *et al*. The contribution of blood lactate to brain energy metabolism in humans measured by dynamic ^{13}C nuclear magnetic resonance spectroscopy. *J Neurosci* 2010; **30**: 13983–13991.
- Lanz B, Xin L, Millet P, Gruetter R. In vivo quantification of neuro-glial metabolism and glial glutamate concentration using ^1H -[^{13}C] MRS at 14.1T. *J Neurochem* 2014; **128**: 125–139.
- Gruetter R, Seaquist ER, Ugurbil K. A mathematical model of compartmentalized neurotransmitter metabolism in the human brain. *Am J Physiol Endocrinol Metab* 2001; **281**: E100–E112.
- Mason GF, Pan JW, Chu WJ, Newcomer BR, Zhang Y, Orr R *et al*. Measurement of the tricarboxylic acid cycle rate in human grey and white matter in vivo by ^1H -[^{13}C] magnetic resonance spectroscopy at 4.1T. *J Cereb Blood Flow Metab* 1999; **19**: 1179–1188.
- Mason GF, Gruetter R, Rothman DL, Behar KL, Shulman RG, Novotny EJ. Simultaneous determination of the rates of the TCA cycle, glucose utilization, alpha-ketoglutarate/glutamate exchange, and glutamine synthesis in human brain by NMR. *J Cereb Blood Flow Metab* 1995; **15**: 12–25.

Supplementary Information accompanies the paper on the Journal of Cerebral Blood Flow & Metabolism website (<http://www.nature.com/jcbfm>)